# Обзор ArXiv:astro-ph, 4-8 марта 2019 года

От Сильченко О.К.

# ArXiv: 1903.02024

# H I galaxies with little star formation: an abundance of LIERs.

Vaishali Parkash,[1]★ Michael J.I. Brown,[1] T. H. Jarrett[2] A. Fraser-McKelvie[3] M.E. Cluver

[1] *School of Physics and Astronomy, Monash Centre for Astrophysics (MoCA), Monash University, Clayton, Victoria 3800, Australia*
[2] *Astrophysics, Cosmology and Gravity Centre (ACGC), Astronomy Department, University of Cape Town, Private Bag X3, Rondebosch 7701, So*
[3] *School of Physics and Astronomy, University of Nottingham, University Park, Nottingham, NG7 2RD, UK*
[4] *Centre for Astrophysics and Supercomputing, Swinburne University of Technology, John Street, Hawthorn, 3122, Australia*
[5] *Department of Physics and Astronomy, University of the Western Cape, Robert Sobukwe Road, Bellville, 7535, South Africa*

Accepted 2019 February 23. Received 2019 February 18; in original form 2018 December 11.

**ABSTRACT**

We present a sample of 91 H I galaxies with little or no star formation, and discuss the analysis of the integral field unit (IFU) spectra of 28 of these galaxies. We identified H I galaxies from the H I Parkes All-Sky Survey Catalog (HICAT) with Wide-field Infrared Survey Explorer (WISE) colours consistent with low specific star formation ($< 10^{-10.4}$ yr$^{-1}$), and obtained optical IFU spectra with the Wide-Field Spectrograph

# Выборка

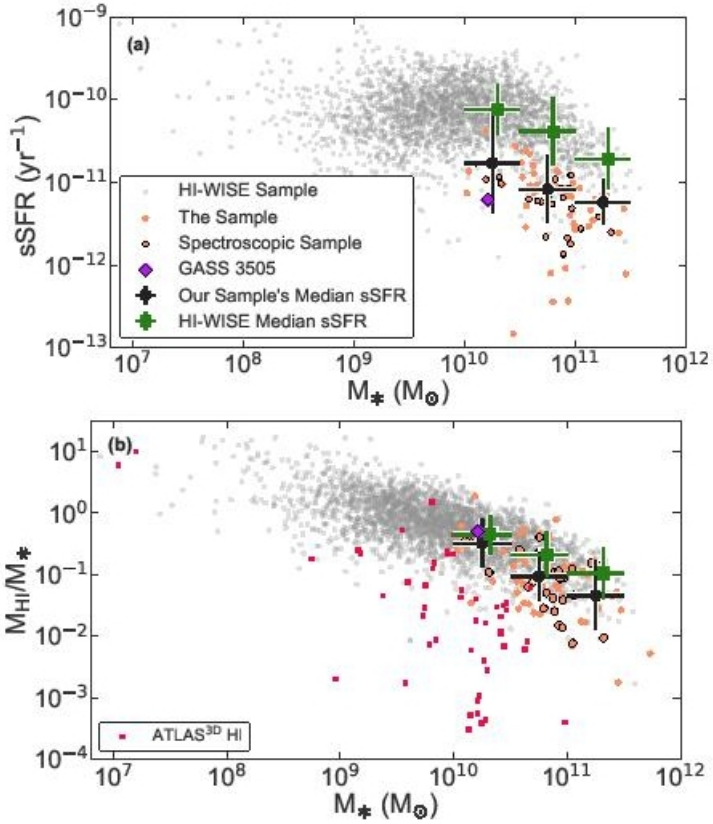


**Figure 2.** The stellar and gas properties of the H I galaxies in the sample compared to the H I-WISE sample: a. sSFR (SFR/$M_*$) versus stellar mass and b. H I mass fraction ($M_{HI}/M_*$) versus stellar mass. Median values are shown for the sample (black circles) and the H I-WISE sample (green squares). Medians for the H I-WISE sample were estimated using only galaxies that met the last three sample selection criteria. For comparison, we also plot the H I and stellar properties of well studied galaxy GASS 3503

- Масса HI – по обзору HIPASS: Нормальная для их звездной массы.
- А вот SFR – ниже главной последовательности в среднем в 2 раза.
- Морфологические типы – от эллиптических до Sbc

# Выборка

| | This Work | | H I-WISE Sample | |
|---|---|---|---|---|
| $\log(M_*)$ $M_\odot$ | log sSFR $yr^{-1}$ | $\log(M_{HI}/M_*)$ | log sSFR $yr^{-1}$ | $\log(M_{HI}/M_*)$ |
| 10.25 | -10.8±0.6 | -0.5±0.4 | -10.1±0.3 | -0.3±0.3 |
| 10.75 | -11.1±0.4 | -1.0±0.4 | -10.4±0.4 | -0.7±0.4 |
| 11.25 | -11.2±0.3 | -1.3±0.6 | -10.7±0.4 | -1.0±0.4 |

2016). In Figure 3 we present example postage stamps images from CGS. Of the 91 galaxies in the sample, 62 galaxies have deep optical images from at least one of these three surveys. By visually inspecting the deep optical images of the 62 galaxies, we find that 35 galaxies exhibit bars and/or rings. We also find that 32 of the 62 galaxies show clear evidence of recent star formation, including blue spiral arms or rings from the deep optical images at large radii (on average $\sim 1'$, or ~10 kpc at $z = 0.01$, but up to ~30 kpc). Excluding those galaxies that show clear or tentative evidence of star formation in deep optical or GALEX ultraviolet images, we find just 9 galaxies (including HIPASSJ1304-30 and HIPASSJ1459-16) that could potentially be passive. Table A1 provides notes on the morphologies and evidence for star formation for individual galaxies, along with redshifts, stellar masses and H I masses.

## 3 SPECTROSCOPIC OBSERVATIONS AND DATA REDUCTION

### 3.1 WiFeS Observations

We observed 28 galaxies from the sample using the Wide Field Spectrograph (WiFeS, Dopita et al. 2007, 2010) integral field unit (IFU) on the Australian National University's

- Всего изначально было выбрано 91 галактика;
- А вот с подвыборкой для спектральных наблюдений на WiFeS 2.3 m Англо-австралийского телескопа – полный сумбур.


**Figure 3.** CGS cutout gri images (CGS; Ho et al. 2011) of 25 galaxies in the sample. The bottom left of each postage stamp includes notes on the optical features of the galaxy such as bars (B), rings (R), star formation in the outer region (SF), edge-on (EO) and dust lanes (DL). Out of these 25 galaxies, 15 exhibit either bar-like, ring-like features or both and 16 galaxies are passive at the centre but show signs of recent star formation in the outskirts. On average, these star-forming rings are ~ 1′ from the centre of the galaxy, which at the sample's average redshift of~ 0.01 corresponds to a radius of ~ 10 kpc. For this work, we have only observed the central 25″ × 38″ region of 28 galaxies with Wide Field Spectrograph (WiFeS, Dopita et al. 2007, 2010) integral field unit (IFU) and therefore do not have observe the faint outer star-forming regions.

# Пассивных всего 9?

# Все-таки расклассифицировали эмиссии ВНЕ ядра…

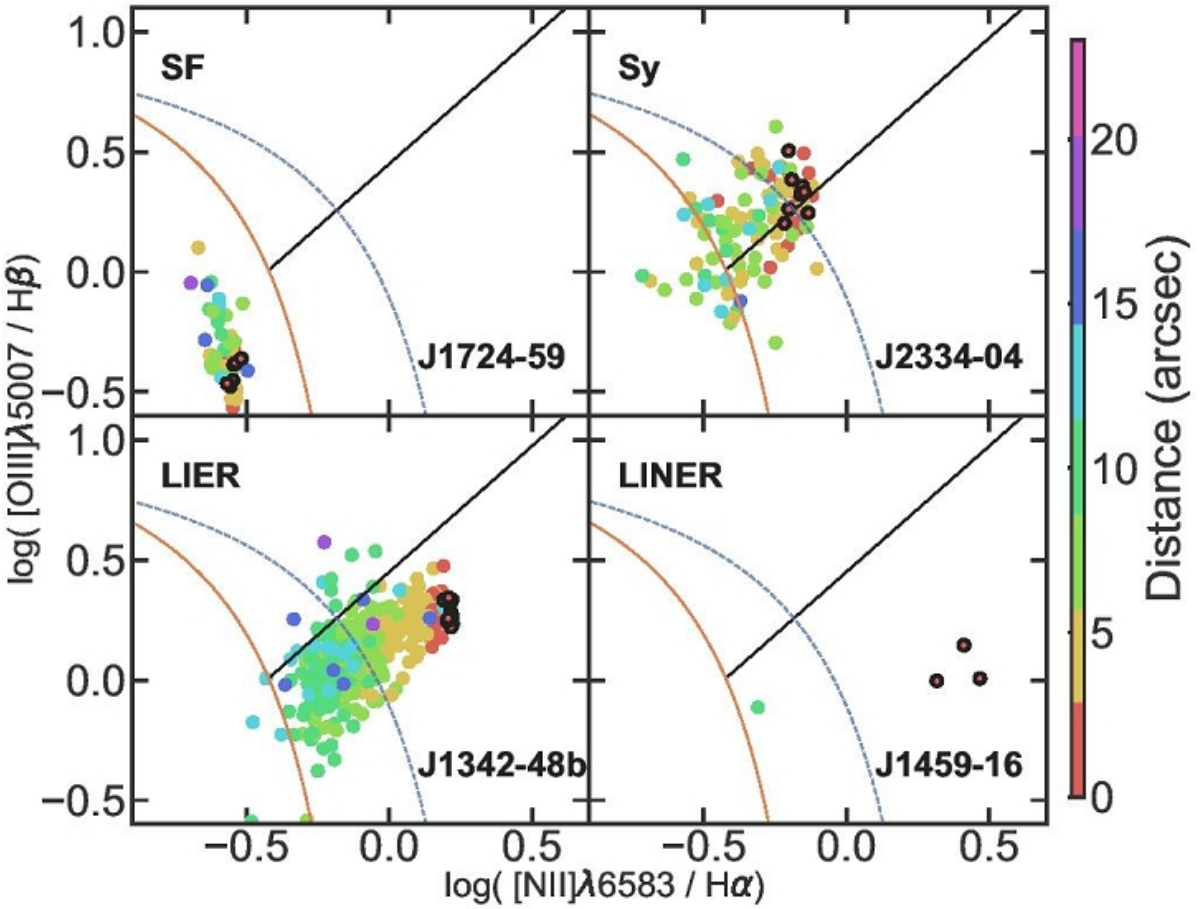


**Figure 7.** Example spatially-resolved BPT emission line ratio diagrams of the different spectroscopic types for the spectroscopic sample. Similar to Figure 5, classification lines are included on each subplot. The colour corresponds to distance between the centre of the Voronoi bin to the galaxy centre. Bins within the central 3″ diameter of the galaxy are circled in black. Only bins with S/N > 3 in all the relevant emission lines are shown. BPT diagrams for the remaining galaxies are given in Appendix C. Out of the 21 galaxies to show central LINER emission in Figure 5, 20 galaxies show emission that extends beyond 3″, so we classify these galaxies as LIERs.

# … большинство оказалось LIERами

**Table 2.** WiFeS observations of 28 galaxies in the sample.

| HIPASS ID | Name | RA (J2000) | DEC (J2000) | z | Obs Date | $D^a_{4000}$ | Age[b] (Gyr) | $\log_{10}([\mathrm{N\ II}]/\mathrm{H}_\alpha)^c$ | $\log_{10}([\mathrm{O\ III}]/\mathrm{H}_\beta)^c$ | Spectral[d] Type |
|---|---|---|---|---|---|---|---|---|---|---|
| 0150-47 | ESO 245-G006 | 01:50:28.7 | -47:09:57 | 0.0207 | 9 July 2018 | 1.85 | 4.32 | 0.082 | 0.1890 | LIER |
| 0154-00b | UGC 01382 | 01:54:41.0 | -00:08:36 | 0.0192 | 22 July 2017 | 1.94 | 6.43 | -0.075 | 0.266 | LIER |
| 0243-29 | NGC 1079 | 02:43:44.3 | -29:00:12 | 0.0048 | 8 August 2018 | 1.60 | 1.87 | -0.314 | -0.125 | LIER |
| 0319-26 | NGC 1302 | 03:19:51.2 | -26:03:38 | 0.0057 | 9 August 2018 | 1.79 | 3.12 | 0.034 | 0.462 | LIER |
| 0330-33 | NGC 1350 | 03:31:08.1 | -33:37:43 | 0.0063 | 11 July 2018 | 1.88 | 4.99 | 0.141 | 0.541 | LIER |
| 0409-56 | NGC 1533 | 04:09:51.8 | -56:07:06 | 0.0026 | 7 August 2018 | 1.96 | 6.97 | 0.302 | 0.403 | LIER |
| 0412-57 | NGC 1543 | 04:12:43.2 | -57:44:17 | 0.0039 | 6 August 2018 | 1.94 | 6.48 | -0.273 | 0.188 | Sy |
| 1251-26 | ESO 507-G025 | 12:51:31.8 | -26:27:07 | 0.0108 | 11 July 2018 | 1.89 | 5.11 | 0.103 | 0.045 | LIER |
| 1301-35 | ESO 381-G047 | 13:01:05.4 | -35:37:00 | 0.0161 | 10 July 2018 | 1.91 | 5.42 | 0.042 | 0.131 | LIER |
| 1321-27 | NGC 5101 | 13:21:46.2 | -27:25:50 | 0.0062 | 9 July 2018 | 1.96 | 6.94 | 0.361 | 0.505 | LIER |
| 1342-48b | NGC 5266 | 13:43:02.1 | -48:10:10 | 0.0100 | 9 July 2018 | 1.98 | 7.27 | 0.212 | 0.275 | LIER |
| 1459-16 | NGC 5796 | 14:59:24.1 | -16:37:26 | 0.0095 | 21 July 2017 | 1.96 | 6.82 | 0.380 | 0.0551 | LINER |
| 1503-13 | MCG-02-38-030 | 15:03:00.2 | -13:16:58 | 0.0084 | 7 August 2018 | 1.82 | 3.71 | 0.177 | 0.572 | LIER |
| 1724-59 | ESO 138-G 024 | 17:24:06.5 | -59:22:56 | 0.0096 | 9 August 2018 | 1.26 | 0.37 | -0.545 | -0.396 | SF |
| 1758-53 | ESO 182-G001 | 17:58:42.7 | -53:47:59 | 0.0119 | 8 August 2018 | 1.87 | 4.79 | 0.128 | 0.378 | LIER |
| 1914-62 | IC 4831 | 19:14:43.8 | -62:16:21 | 0.0145 | 6 August 2018 | 1.82 | 3.84 | 0.112 | 0.533 | LIER |
| 1932-55 | NGC 6799 | 19:32:16.5 | -55:54:29 | 0.0112 | 7 August 2018 | 1.83 | 3.98 | -0.056 | 0.231 | LIER |
| 1945-54 | IC 4889 | 19:45:15.1 | -54:20:39 | 0.0086 | 20 July 2017 | 1.87 | 4.74 | 0.175 | 0.364 | LIER |
| 2013-37 | ESO 399-G025 | 20:13:27.7 | -37:11:20 | 0.0085 | 12 July 2018 | 1.95 | 6.65 | -0.512 | 0.486 | Sy |
| 2015-21 | ESO 596-G012 | 20:15:43.5 | -21:30:59 | 0.0196 | 11 July 2018 | 1.65 | 2.22 | -0.129 | 0.260 | LIER |
| 2018-16 | IC 1313 | 20:18:43.6 | -16:56:45 | 0.0110 | 5 August 2018 | 1.89 | 5.18 | 0.066 | 0.440 | LIER |
| 2118-63 | IC 5096 | 21:18:21.5 | -63:45:38 | 0.0105 | 6 August 2018 | 1.92 | 5.68 | 0.009 | 0.276 | LIER |
| 2153-37 | 2MASXJ21525329-3739110 | 21:52:53.3 | -37:39:11 | 0.0149 | 25 August2018 | 1.80 | 3.38 | -0.187 | 0.817 | Sy |
| 2201-31 | ESO 466-G036 | 22:01:20.4 | -31:31:47 | 0.0079 | 8 August 2018 | 1.35 | 0.54 | -0.920 | 0.413 | SF |
| 2224-03 | MCG-01-57-004 | 22:23:39.1 | -03:25:54 | 0.0094 | 9 August 2018 | 1.63 | 2.05 | -0.62 | -0.210 | SF |
| 2241-44 | IC 5240 | 22:41:52.4 | -44:46:02 | 0.0059 | 9 July 2018 | 1.71 | 2.73 | -0.011 | 0.158 | LIER |
| 2243-64 | IC 5244 | 22:44:13.7 | -64:02:36 | 0.0116 | 8 August 2018 | 1.95 | 6.65 | 0.0178 | 0.362 | LIER |
| 2334-04 | IC 5334 | 23:34:36.4 | -04:32:03 | 0.0074 | 8 August 2018 | 1.82 | 3.68 | -0.167 | 0.319 | Sy |

[a] Calculated using the narrow definition of Balogh et al. (1999).
[b] Based on Bruzual & Charlot (2003) models using Chabrier (2003) IMF and assuming Solar metallicity.
[c] Emission line ratios measured from the integrated spectra composed of spaxels within a 1.5″ radius from the centre of the galaxy. We refer to [O III]$\lambda$ 5007 Å and [N II]$\lambda$ 6583 Å as [O III] and [N II], respectively.
[d] AGN classification for the sample following the definition of Kauffmann et al. (2003) and Schawinski et al. (2007). Sy = Seyfert, LINER = low-ionisation nuclear emission-line region, LIER = low-ionisation emission-line region, SF = Star forming or H II regions.